Supplementary Material

Primary Title: Decadal Trends and Suspended Sediment Fluxes in the Upper Blue Nile: Sedigraph Reconstruction and Coupled Hydro-Sediment Modelling

Original Abstract Title: Suspended Sediment Fluxes and Decadal Trends in the Humid Tropics: Machine Learning Reconstruction and Coupled Modelling in Upper Blue Nile Tributaries

Abstract ID: EGU26-4157

Authors: Kindie B. Worku, Fasikaw A. Zimale, Till Francke, Morteza Zargar, and Axel Bronstert

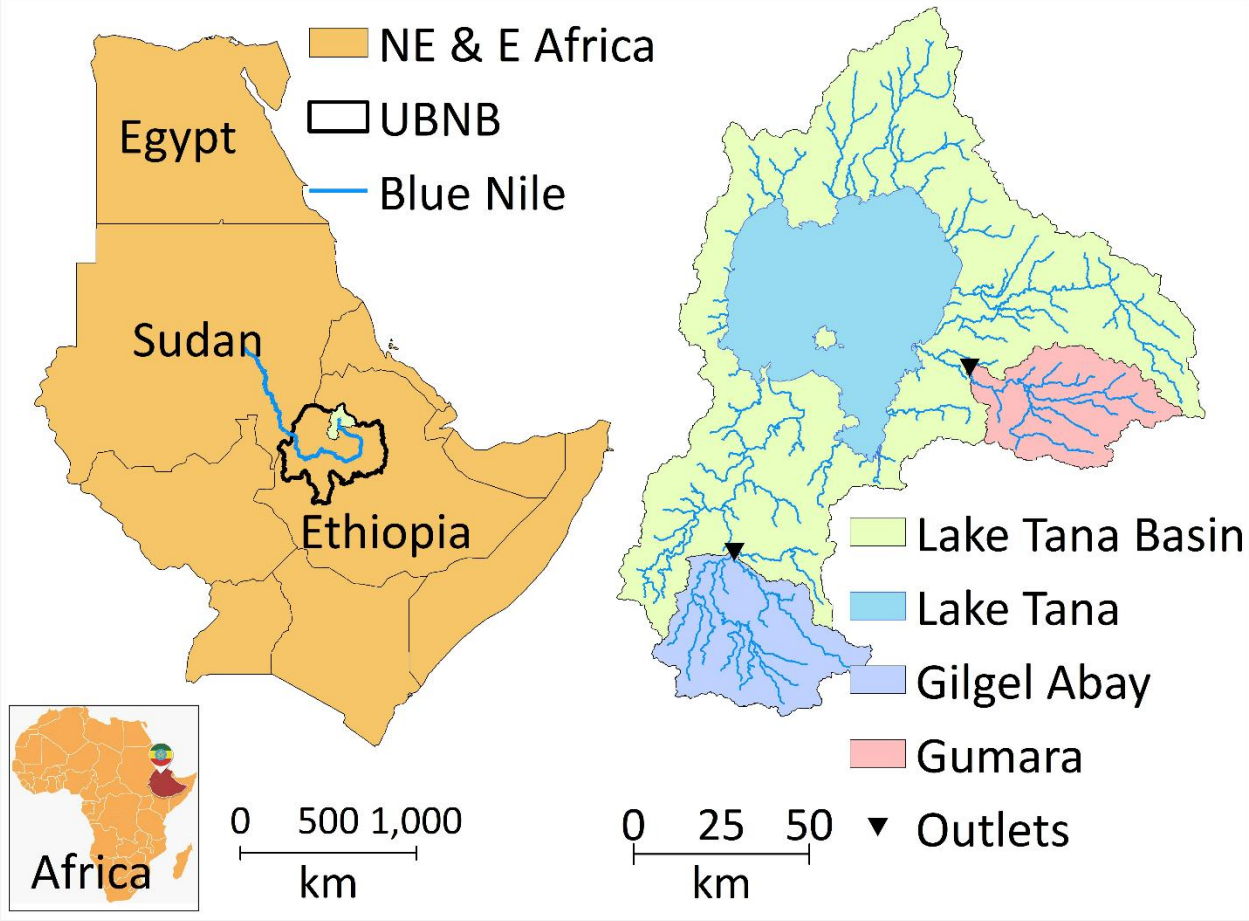

Figure S1. Location and spatial extent of the study area. Regional setting of the Upper Blue Nile Basin (UBNB) within northeastern and eastern Africa, including national boundaries and the Blue Nile River, as well as a detailed map of the Lake Tana Basin showing Lake Tana, the Gilgel Abay and Gumara tributary catchments, river networks, and outlet locations.

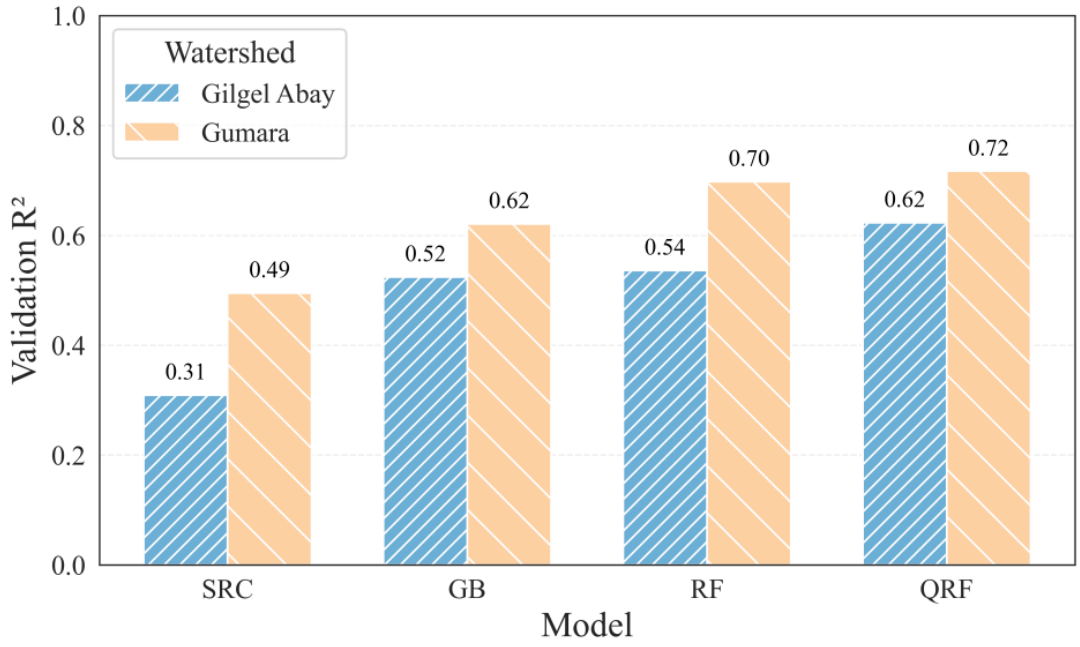

Figure S2. Comparison of model performance based on validation R^2 for SSC Prediction Models (SRC, GB, RF, QRF) in Gilgel Abay and Gumara (1990–2020). SRC: Sediment Rating Curve; GB: Gradient Boosting; RF: Random Forest; QRF: Quantile Random Forest; SSC: Suspended Sediment Concentration.

Table S1. Model performance in predicting suspended sediment concentration in the Gilgel Abay and Gumara watersheds (1990–2020) using Sediment Rating Curve (SRC), Gradient Boosting (GB), Random Forest (RF), and Quantile Random Forest (QRF). Metrics include training and validation coefficient of determination (R^2), mean absolute error (MAE), root mean squared error (RMSE), and mean absolute percentage error (MAPE). The QRF model achieved the highest accuracy across both watersheds.

Watershed	Model	R^2	Validation R^2	RMSE(g/L)	MAE(g/L)	MAPE(%)
Gilgel Abay	SRC	0.32	0.31	0.67	1.48	27.84
	GB	0.85	0.52	0.63	1.23	31.39
	RF	0.74	0.54	0.67	1.21	29.35
	QRF	**0.89**	**0.62**	**0.52**	**1.09**	**20.44**
Gumara	SRC	0.40	0.50	0.35	0.54	22.58
	GB	0.89	0.62	0.31	0.47	24.57
	RF	0.85	0.70	0.28	0.42	21.16
	QRF	**0.94**	**0.72**	**0.27**	**0.41**	**16.34**

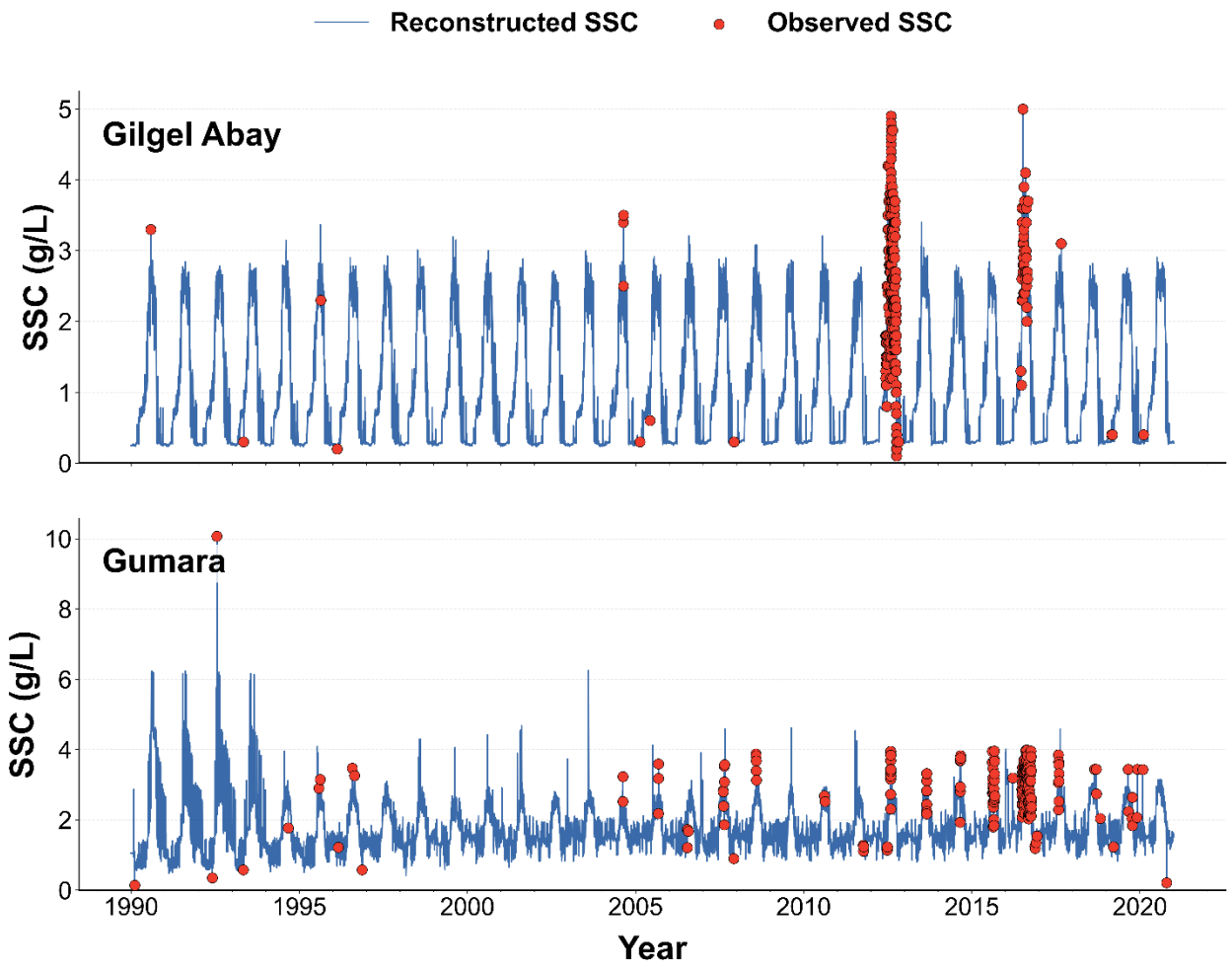

Figure S3. Full reconstructed vs. observed Suspended Sediment Concentration (SSC) time series (1990–2020) for Gilgel Abay (top) and Gumara (bottom). The daily reconstructed SSC (solid blue line) was generated using the Quantile Regression Forests (QRF) approach to fill the extensive temporal gaps in the direct grab-sample measurements (red dots). This 31-year reconstructed record demonstrates strong representation of the basin's response to rapid monsoon flows. It provides the continuous sediment baseline required to evaluate the long-term, diverging hydrological regimes and cumulative wetland loss impacts observed in the catchments.

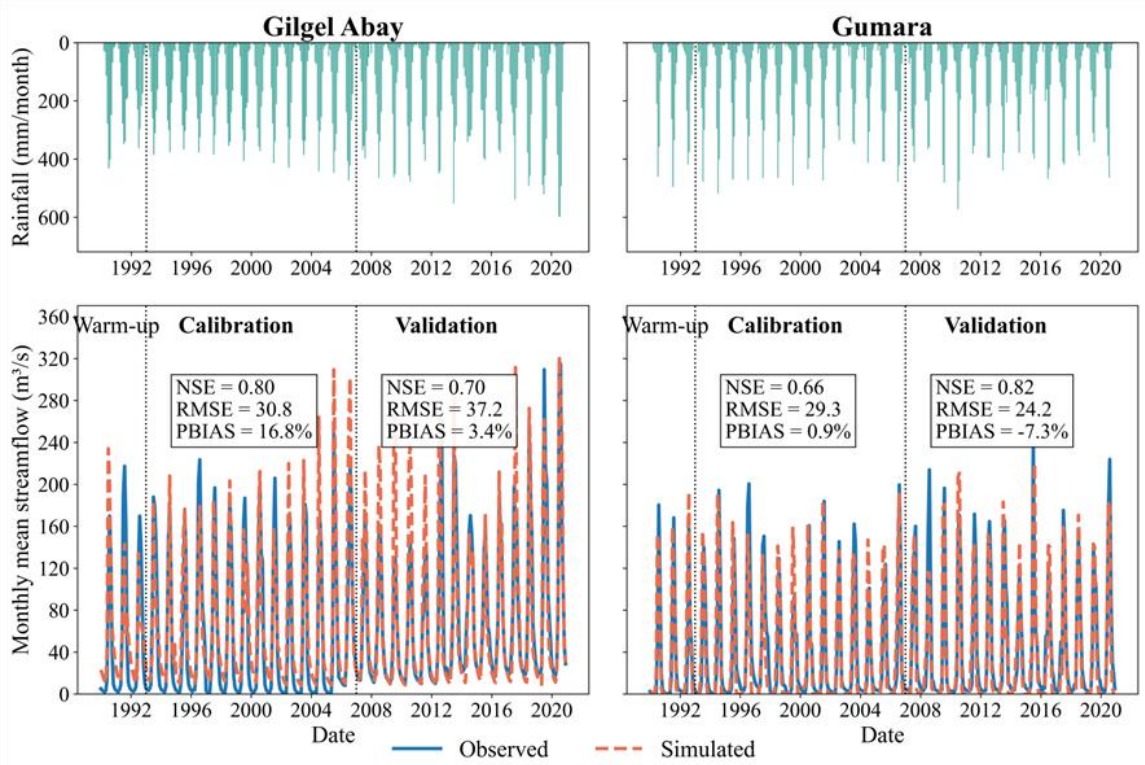

Figure S4. Monthly rainfall (top) and observed vs. simulated streamflow (bottom) for the Gilgel Abay and Gumara watersheds from 1990 to 2020 using WASA-SED model. Rainfall is plotted with an inverted axis to align visually with streamflow responses. Vertical dashed lines mark the warm-up (1990–1992), calibration (1993–2006), and validation (2007–2020) periods. Model performance is summarized using NSE, RMSE, and PBIAS, showing good agreement during calibration and consistent behavior in validation.

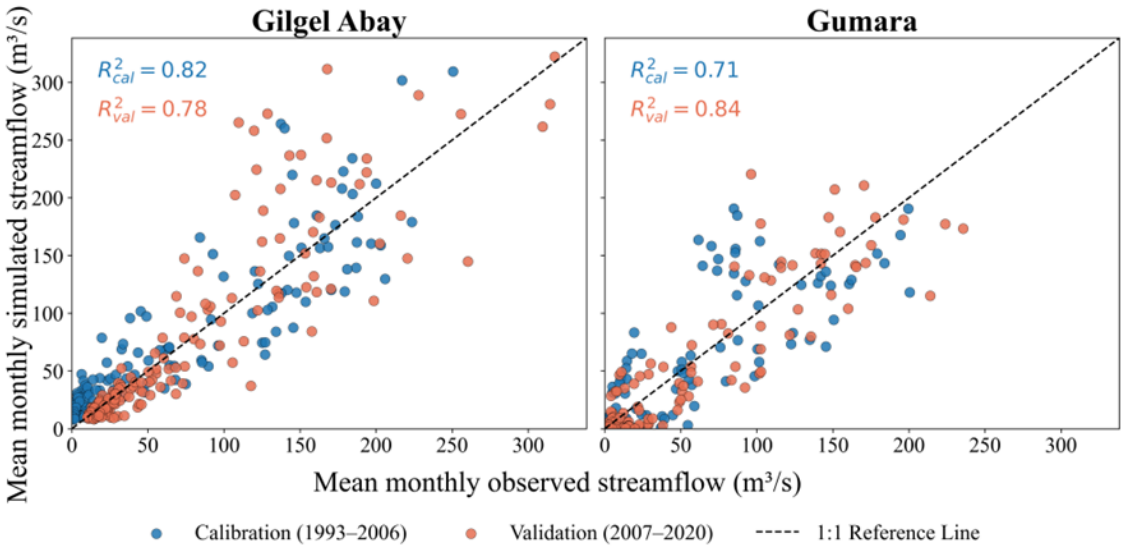

Figure S5. Scatter plots comparing observed and simulated monthly streamflow for the Gilgel Abay and Gumara watersheds during calibration (1993–2006) and validation (2007–2020) periods. The coefficient of determination (R^2) quantifies the model's performance for each period.

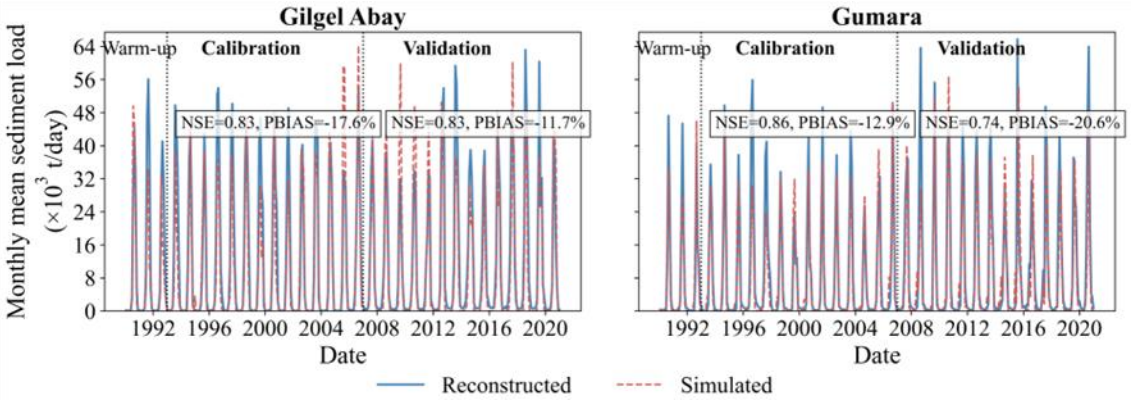

Figure S6. Reconstructed and simulated monthly sediment load (×10^3 t/day) for the Gilgel Abay (left) and Gumara (right) watersheds during the warm-up (1990–1992), calibration (1993–2006), and validation (2007–2020) periods using WASA-SED. The Sedigraph illustrates seasonal sediment dynamics and model performance across the simulation periods.

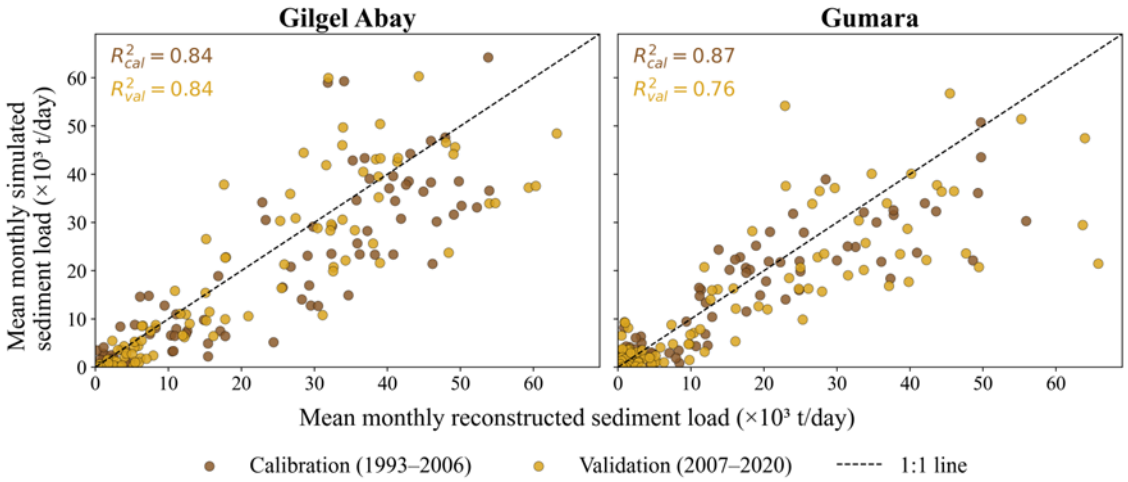

Figure S7. Reconstructed versus modelled monthly mean sediment load during the calibration (1993–2006) and validation (2007–2020) periods for the Gilgel Abay and Gumara watersheds. The coefficient of determination (R^2) quantifies the model's performance for each period.

Table S2. Land-use and Land-cover (LULC) changes in the Gilgel Abay and Gumara watersheds between 2000 and 2020 derived from the Global Land Analysis and Discovery (GLAD) datasets. Area values are in km^2, with the percentage change reflecting the relative difference over the 20 years.

Watershed	Land Cover Type	Area in 2000 (km^2)	Area in 2020 (km^2)	Change (%)
Gilgel Abay	Cropland	590	551	-6%
	Dense short vegetation	631	527	-16%
	Tree cover	394	469	18%
	Built-up	7.3	76	940%
Gumara	Cropland	875	882	0%
	Dense short vegetation	304	261	-14%
	Tree cover	178	190	6%
	Built-up	4.6	32	580%
	Wetland	4.4	1.6	-63%

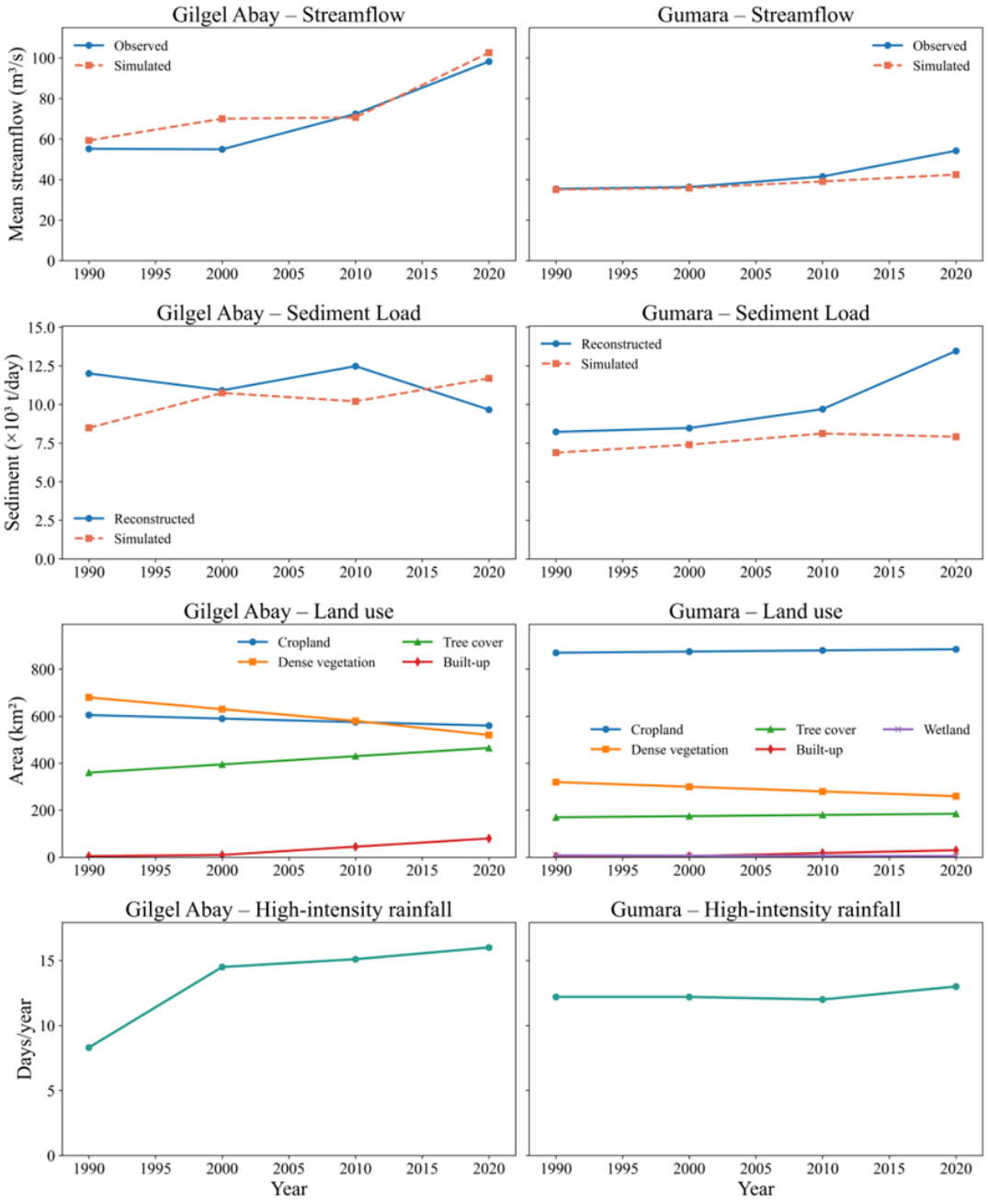

Figure S8. Decadal dynamics in the Gilgel Abay and Gumara watersheds (1990–2020). Panels display (top row) mean streamflow (observed, solid; simulated, dashed), (second row) sediment load (×10^3 t/day), (third row) land-use area (km^2), and (bottom row) number of high-intensity rainfall days (>20 mm/day). Streamflow and sediment are shown as discrete segments representing independent decadal means, whereas land-use and rainfall extremes are connected to illustrate temporal evolution. Values represent decadal means or aggregates for the four periods (1990s, 2000s, 2010s, and 2020s).

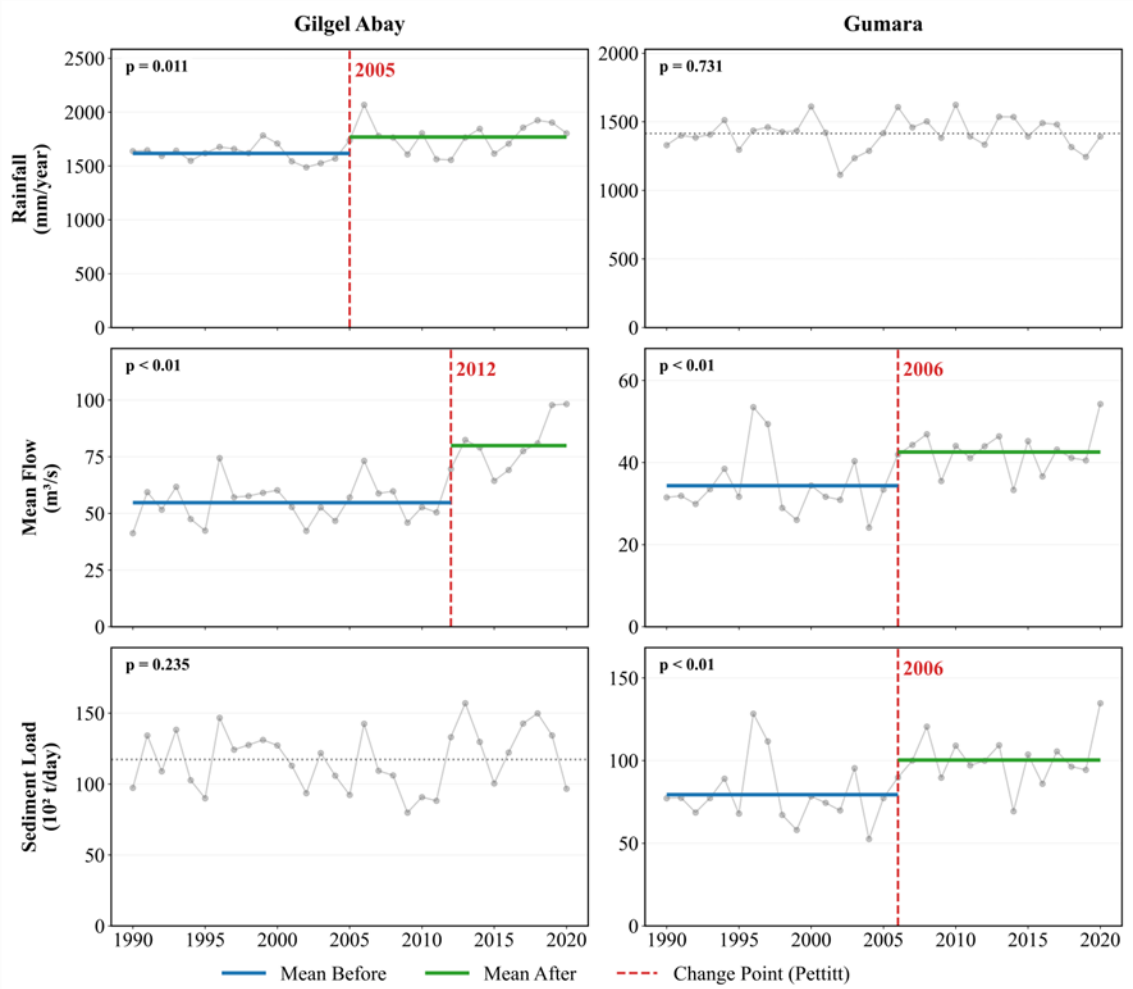

Figure S9. Annual time series of rainfall (mm/year), mean streamflow (m^3/s), and mean sediment load ($\times 10^2$ t/day) for the Gilgel Abay (left column) and Gumara (right column) watersheds over 1990–2020. Blue and green horizontal lines represent mean values before and after the detected change point, respectively. Red dashed vertical lines mark the year of the significant change point identified by the Pettitt test, with corresponding p-values shown in each panel.